

LATTICE COMPARISON FOR THE 8 GeV SYNCHROTRON RADIATION SOURCE

K. Tsumaki, R. Nagaoka, K. Yoshida, H. Tanaka and M. Hara
RIKEN-JAERI Synchrotron Radiation Facility Design Team
2-28-8, Honkomagome, Bunkyo-ku, Tokyo, 113, Japan

Abstract

Chasman-Green (CG), Triple Bend Achromat (TBA) and Quadruple Bend Achromat (QBA) lattice have been designed and the dynamic characteristics of these three lattices have been studied for the lattice selection of the 8 GeV low emittance synchrotron radiation source. The results showed that each lattice had both merits and demerits and the absolute superiority or inferiority between the lattices was not recognized so far as the dynamic characteristics were concerned. These results lead us to the conclusion that CG lattice which has the simplest magnet arrangement was suited for the 8 GeV synchrotron radiation source.

Introduction

RIKEN and JAERI, which are supervised by Science and Technology Agency of Japanese Government (STA), are planning to construct the large synchrotron radiation facility [1][2]. The emittance of the storage ring is planned to be less than 10^{-8} m.rad.

Generally, electron beams in a low emittance storage ring are strongly focused to achieve low emittance and this fact generates many problems which are not principal difficulty for a high emittance storage ring. The dynamic aperture of such low emittance storage ring is too small and the sensitivity against the field errors is very high. We then need to design the storage ring which overcomes these problems.

Chasman-Green lattice [3] which has two bending magnets in a cell and Triple Bend Achromat lattice [4] which has three bending magnets in a cell are well known as a low emittance lattice for synchrotron radiation source. In addition to these lattices, we designed a Quadruple Bend Achromat lattice (QBA) which had four bending magnets in a cell and the dynamic characteristics of these three lattices were studied. On the basis of these studies, we compared the dynamic characteristics to select the suitable lattice for the 8 GeV low emittance storage ring for synchrotron radiation source.

Table 1 Ring parameters and number of magnets

| | CG | TBA | QBA |
|--------------------------|---------|---------|---------|
| Emittance (nm.rad) | 4.9 | 5.8 | 5.0 |
| Tune ν_x | 51.75 | 48.76 | 49.6 |
| ν_y | 19.82 | 26.39 | 19.60 |
| Circumference (m) | 1478.4 | 1477.8 | 1476.5 |
| No. of cells | 48 | 36 | 32 |
| Dipole magnet (per cell) | 96(2) | 108(3) | 128(4) |
| Quadrupole magnet | 480(10) | 432(12) | 480(15) |
| Sextupole magnet | 336(7) | 216(6) | 288(9) |

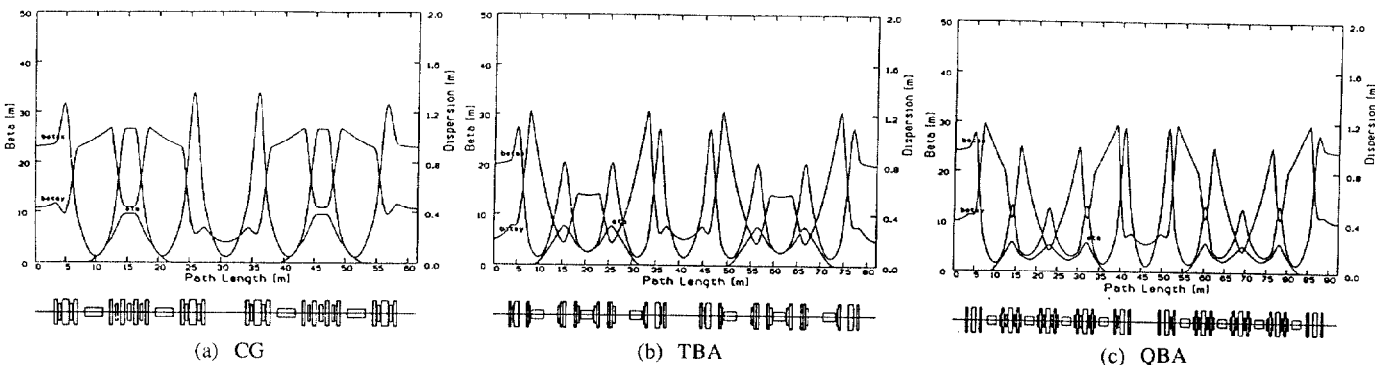


Fig. 1 Lattice functions of one superperiod.

Lattice Design

Linear Optics

To compare the characteristics on the same boundary condition, we imposed the following conditions in designing the lattices.

- The electron energy is 8 GeV and the bending magnet field strength is 0.6 T.
- Emittance is less than 5×10^{-9} m.rad.
- Circumference is less than 1500 m.
- Number of straight sections is more than 32.
- The length of the straight section is 6.5 m.
- Horizontal beta function is alternately high and low.

Figure 1 shows the lattice functions which are designed on the basis of above conditions. Table 1 shows the ring parameters and the number of magnets.

Dynamic Aperture

The dynamic apertures of each storage ring are shown by square mark in Fig. 2. These small dynamic apertures are mainly dominated by the first and third order resonances which are induced by the strong sextupole fields of chromaticity correction sextupole magnets. To avoid these resonances, the amplitude dependent tune shift should be suppressed to small values. According to the perturbation theory, the amplitude dependent tune shifts in a superperiod are given by ,

$$\Delta\nu_{xc} = C_{11}2J_x + C_{12}2J_y \tag{1}$$

$$\Delta\nu_{yc} = C_{21}2J_x + C_{22}2J_y \tag{2}$$

where

$$x = \sqrt{2J_x\beta_x} \cos\phi_x, \quad y = \sqrt{2J_y\beta_y} \cos\phi_y$$

and $J_x(J_y)$ and $\phi_x(\phi_y)$ denote the action and angle variable, respectively. Coefficients C_{ij} are expressed by eqs.(3),(4),(5).

$$C_{11} = -18\Sigma_m \{ A_{3m}^2 / (3\nu_{xc}-m) + 3A_{1m}^2 / (\nu_{xc}-m) \} \tag{3}$$

$$C_{12} = C_{21} = 36\Sigma_m \{ 2B_{1m}A_{1m} / (\nu_{xc}-m) - B_{+m}^2 / (\nu_{xc}+2\nu_{yc}-m) + B_{-m}^2 / (\nu_{xc}-2\nu_{yc}-m) \} \tag{4}$$

$$C_{22} = -18\Sigma_m \{ 4B_{1m}^2 / (\nu_{xc}-m) + B_{+m}^2 / (\nu_{xc}+2\nu_{yc}-m) + B_{-m}^2 / (\nu_{xc}-2\nu_{yc}-m) \} \tag{5}$$

where ν_{xc} and ν_{yc} are the tune for one superperiod.

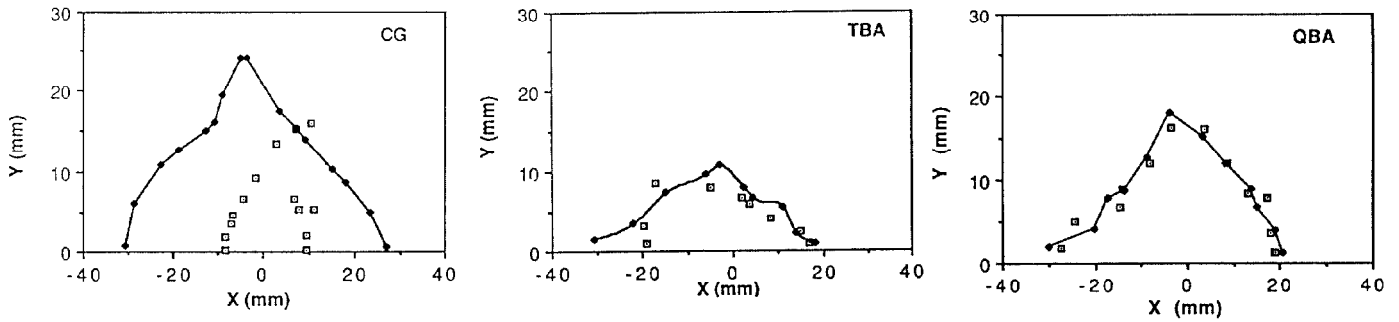


Fig. 2 Dynamic aperture (□: without harmonic sextupoles, ◆: with harmonic sextupoles).

A_{1m}, A_{3m}, B_{1m} and B_{\pm} are expressed by eqs. (6),(7),(8),(9).

$$A_{1m} = \Sigma_k (S_k/48\pi) \beta_x^{3/2} \cos(\int 1/\beta_x ds - \nu_{xc}\theta + m\theta) \quad (6)$$

$$A_{3m} = \Sigma_k (S_k/48\pi) \beta_x^{3/2} \cos(3(\int 1/\beta_x ds - \nu_{xc}\theta) + m\theta) \quad (7)$$

$$B_{1m} = \Sigma_k (S_k/48\pi) \beta_x^{1/2} \beta_y \cos(\int 1/\beta_x ds - \nu_{xc}\theta + m\theta) \quad (8)$$

$$B_{\pm m} = \Sigma_k (S_k/48\pi) \beta_x^{1/2} \beta_y \cos\{\int (1/\beta_x \pm 2/\beta_y) ds - (\nu_{xc} \pm 2\nu_{yc})\theta + m\theta\}$$

where S_k is the strength of sextupole magnets. (9)

As we can see in eqs. (3),(4),(5), the first and the third order resonances driven by the sextupole fields are,

$$\nu_{xc} = N, \quad 3\nu_{xc} = N, \quad \nu_{xc} + 2\nu_{yc} = N. \quad (10)$$

In CG lattice, ν_{xc} is 2.16. This means that $m=6$ or 7 in the first term in eq. (3) (A_{36} or A_{37} term) and $m=2$ in the second term of eq. (3) and in the first term of eq. (4) (A_{12} or B_{12} term) are the most harmful. Harmonic expansion spectrums of C_{ij} and the dynamic aperture prediction in the single resonance approximation by CATS [5] showed that A_{12} and A_{37} term gave the limitation of dynamic aperture. Therefore, A_{12} and A_{37} term were suppressed by the additional sextupole magnets (harmonic sextupoles). The strength of the harmonic sextupoles were also optimized by CATS. Similarly, we knew that the major term which gave the limitation of dynamic aperture in TBA lattice were A_{12} and A_{37} . However, we failed simultaneous suppression of A_{12} and A_{37} term. This is obvious from Fig. 3. In case of CG lattice, the position dependence of A_{12} and A_{37} which we denote A'_{12} and A'_{37} show the same behavior. This means that A_{12} and A_{37} only with chromaticity correction sextupoles have the same sign. Therefore, we can suppress A_{12} and A_{37} by setting the harmonic sextupoles in the non-dispersive section where A'_{12} and A'_{37} have the same sign. In case of TBA lattice, the signs of A'_{12} and A'_{37} in the dispersive section are different. Then A_{12} and A_{37} only with chromaticity correction sextupoles have the different

sign. While, the signs of A'_{12} and A'_{37} in non-dispersive section are the same. This means that A_{12} and A_{37} can not be suppressed simultaneously by the harmonic sextupoles which are set in non-dispersive section. In case of QBA lattice, the harmful harmonics were A_{13} and A_{39} . The signs of A'_{13} and A'_{39} in dispersive section are different but they are different in non-dispersive low beta section. We can then suppress A_{13} and A_{39} simultaneously. However, if we suppress A_{13} and A_{39} to the extent, where A_{13} and A_{39} are not the main source of dynamic aperture limitation, the other harmonics grow and give the dynamic aperture limitation. Consequently, the dynamic aperture can not be enlarged by the harmonic sextupoles. This situation that if we suppress the particular harmonics, the other harmonics grow and give the dynamic aperture limitation is more or less true for CG lattice. But in case of TBA and QBA lattice, the situation is more serious and complex than CG lattice. Solid lines in Fig. 2 show the dynamic apertures enlarged by this method.

Lattice Comparison

Lattice characteristics greatly depend on the degree of optimization and it is very difficult to extract a universal trend. Nevertheless, we compared the dynamic characteristics of the lattice to select the suitable lattice for the 8 GeV storage ring. Compared items are the dynamic aperture size and the sensitivity against the errors.

Dynamic Aperture

We evaluated not only the dynamic aperture for the ideal lattice but also for the realistic lattice which have various kinds of errors. Particle trackings with errors were done by RACETRACK [6]. If the magnets have various errors, the closed orbit distortions(COD) occur. Therefore, we evaluated the dynamic aperture size as a function of COD, which can be varied by the degree of COD correction. Table 2 shows the error conditions. Tracking results for the ideal machine and for the machine with errors are shown in Fig. 2 and Fig. 4, respectively. Three machines have enough dynamic aperture if the errors are not taken into account. However, the dynamic aperture size reduces to less than 2/3 even if the COD is corrected completely. For TBA and QBA lattice, aperture size is almost the same size which is needed for injection.

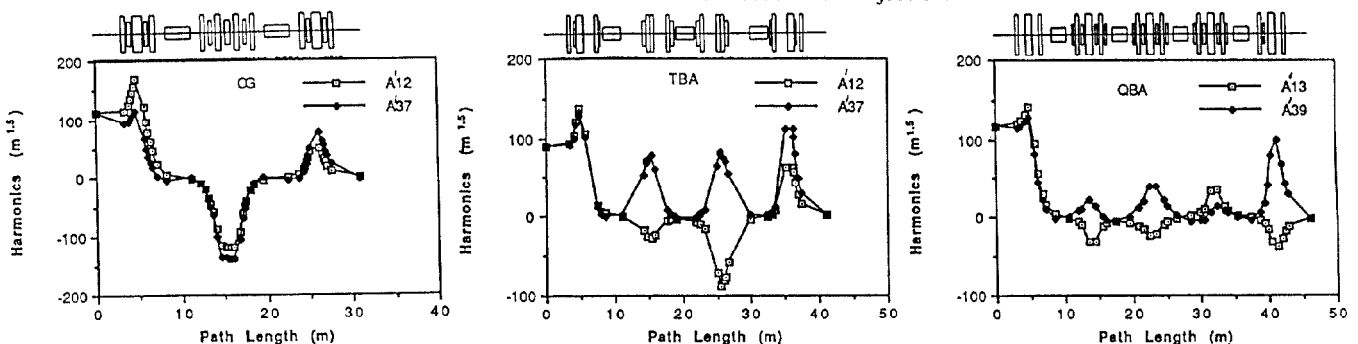


Fig. 3 Position dependence of harmonics in a cell.

Table 2 Error conditions

| | Item | Strength |
|-------------------|---------------------------------------|--------------------|
| Dipole magnet | Field error $ \Delta B/B $ | 5×10^{-4} |
| | Rotation error $ \Delta \theta $ | 0.5 mrad |
| Quadrupole magnet | Misalignment $ \Delta x , \Delta y $ | 0.2 mm |
| | Gradient error $ \Delta k/k $ | 5×10^{-4} |
| | Tilt error $ \Delta \theta $ | 0.5 mrad |
| Sextupole magnet | Misalignment $ \Delta x , \Delta y $ | 0.2 mm |
| | Gradient error $ \Delta k/k $ | 5×10^{-4} |
| | Tilt error $ \Delta \theta $ | 0.5 mrad |

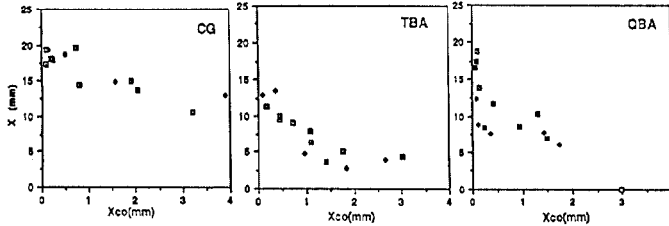


Fig. 4 Horizontal dynamic aperture as a function of closed orbit distortions.

Sensitivity

It is very important for users of synchrotron radiation that the electron beams keep the same condition sufficiently long time. However, if the machine has high sensitivity against the errors, beam condition will easily change. From the stand point of machine designer, such sensitive machine is not favourable. Therefore, we investigated the sensitivity against the errors. The investigated items are the followings.

- Closed orbit distortions X_{co} and Y_{co} arising from the alignment errors of quadrupole magnets.
- Beta value distortions $\Delta\beta/\beta$ arising from field gradient errors of quadrupole magnets $\Delta k/k$ and COD in sextupole magnets.
- Spurious dispersions ΔD arising from the field gradient errors $\Delta k/k$ and tilted errors $\Delta\theta$ of quadrupole magnets and COD in quadrupole and sextupole magnets.

For the calculation of spurious dispersions, the following errors are supposed; $\Delta k/k = 10^{-3}$, $X_{co} = Y_{co} = 1$ mm, $\Delta\theta = 1$ mrad. Evaluation point is the high beta straight section.

Figure 5(a) shows the sensitivity against the alignment errors of quadrupole magnets. From Fig. 5(a), we knew that the sensitivity against the quadrupole magnet alignment errors for CG lattice was the highest of the three lattices and 0.1 mm alignment errors produced 8 mm COD. Figure 5(b) shows that the beta value distortions arising from the gradient errors of quadrupole magnets are almost the same between the three lattices and $\Delta\beta/\beta$ is about 4% ~ 6% for the 0.1% gradient errors. The beta value distortions arising from COD in sextupole magnets are from 2%, which is the case for horizontal distortions for TBA lattice, to 10%, which is vertical distortions for QBA lattice. Vertical beta distortions for QBA lattice is exceptional because the

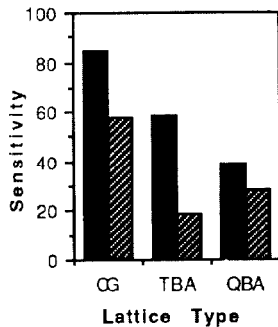


Fig. 5(a) Sensitivity against alignment errors of quadrupoles.

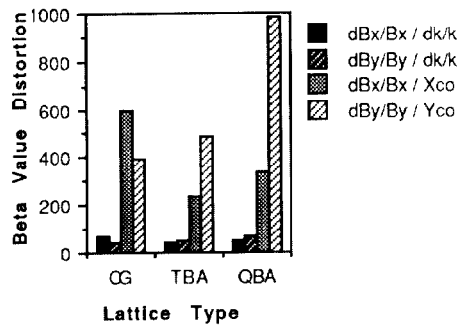


Fig. 5(b) Beta value distortions arising from gradient errors of quadrupoles and COD in sextupoles.

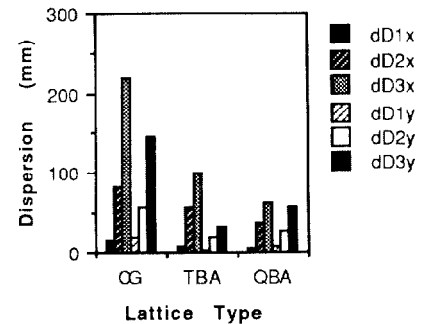


Fig. 5(c) Spurious dispersions arising from field gradient errors and tilted errors of quadrupoles and COD in Quadrupoles and Sextupoles.

sextupole arrangement for chromaticity correction is somewhat different from the other two lattices to enlarge the dynamic aperture. Figure.5(c) shows that the spurious dispersions for CG lattice is the largest in the three lattices. If we assume the 0.1% gradient errors, 0.1 mm COD and 0.5 mrad tilt errors, horizontal and vertical spurious dispersions are 44 mm and 30 mm, respectively.

Summary of Comparison

We knew that the each lattice fulfilled the irreducible minimum requirements as a low emittance storage ring. To compare the dynamic characteristics totally, we summarized the characteristics as shown in Table 3. Table 3 shows us that each lattice has its own merits and demerits and absolute superiority or inferiority does not exist. We then could not have definite reason to determine the lattice type as far as the dynamic characteristics were concerned.

If we apart from the stand point of dynamic characteristics, we can easily know that the lattice which have simplest magnet arrangement and shortest cell length is CG lattice. These results lead us to the conclusion that the most suitable lattice for the 8 GeV low emittance storage ring is CG lattice.

Table 3 Comparison of dynamic characteristics of CG, TBA, and QBA lattice.

| | | CG | TBA | QBA |
|------------------|----------------|----|-----|-----|
| Dynamic aperture | with errors | 1 | 3 | 2 |
| | without errors | 1 | 3 | 2 |
| Sensitivity | C.O.D. | 3 | 2 | 1 |
| | $\Delta\beta$ | 2 | 1 | 3 |
| | $\Delta\eta$ | 3 | 2 | 1 |

Conclusion

Chasman-Green lattice, Triple Bend Achromat lattice and Quadruple Bend Achromat lattice have been designed and the dynamic characteristics have been studied. We could not recognize the absolute superiority of the specific lattice between the three lattices in dynamic characteristics. However, Chasman-Green lattice has the simplest magnet arrangement and the shortest cell length. Accordingly, we determined to choose Chasman-Green lattice as the 8 GeV low emittance storage ring lattice.

References

- [1] M. Hara et al., "Storage Ring Design for STA SR Project", in this conference.
- [2] H. Yokomizo et al., "Injection System for the Large Radiation Facility in Japan", in this conference.
- [3] R. Chasman, G. K. Green and M. Rowe, IEEE Trans. Nucl. Sci. NS-22 (1975) 1765.
- [4] G. Vignola, Nucl. Instrum. & Methods A236 (1985) 414.
- [5] R. Nagaoka et al., RIKEN Accel. Prog. Rep. 1988.
- [6] A. Wrulich : DESY Report-84-026.